First Principles Investigation of the Substitutional Doping of rare-earth elements and Co in La_4MgNi_{19} Phase

Yuchen Liu[1,2], Djafar Chabane[1,2], Omar Elkedim[1,2]

[1] Affiliation 1: FEMTO-ST Institute, Univ. Bourgogne Franche-Comte, UTBM, CNRS, Belfort, France. E-mail: yuchen.liu@utbm.fr

[2] Affiliation 2: FEMTO-ST Institute, FCLAB, Univ. Bourgogne Franche-Comte, CNRS, Belfort, France.

Abstract

RE-Mg-Ni alloys, including AB_3, A_2B_7, A_5B_{19} and AB_4 types, have received extensive attention due to their excellent hydrogen storage properties. La_4MgNi_{19} is the one of the outstanding candidate for hydrogen storage. In this work, The structure, phase stability and electronic structure of the different La-site partial substituted by Pr, Sm, Gd, Nd and NI-site substituted by Co have been investigated by means of the density functional theory.

The calculation results show that La_4MgNi_{19} alloy shows the negative enthalpy of formation, indicating the more stable in the thermodynamic. When the substitution of La occurs, among the two sites La(2c) and La(4f), Pr, Nd, Sm and Gd preferentially occupy the La(4f) site. And the addition of the four doping elements will reduce the stability of the phase. Among them, Pr substituted La_4MgNi_{19} has the highest structural stability. When Co substituting Ni, a single Co atom occupies the Ni(12k) preferentially among the seven different Ni positions. During this process, the crystal structure will be destabilized. The DOS results show that the system still puts up the metallic character after substitution. Sm(La(4f)) has the maximum valence band width. The stability of four doped alloys from high to low is: Pr, Nd, Sm, Gd, which is consistent with the enthalpy of formation results. The enthalpy of formation of hydrides shows that, the bounding hydrogen capacity of the system can be obtained as Nb > Sm > Pr > Gd.

Keyword: Hydrogen energy storage, Rare-earth-based alloys, Total energies, Electronic structure.

1. Introduction

With the continuous consumption and depletion of fossil energy[1], as well as the more and more serious environmental pollution[2], the search for new clean energy has become imminent[3]. As a clean energy, hydrogen energy has incomparable advantages over other clean energy sources, such as solar energy, wind energy, and geothermal energy [4]. But in the process of today's hydrogen economy, hydrogen storage is the biggest hurdle[5]. Lots of traditional or novel methods are applied to store hydrogen(gaseous or atomic)[6], including high-pressure hydrogen storage, ultra-low temperature hydrogen storage, physical adsorption hydrogen storage, and chemical hydrogen storage. Among them, chemical hydrogen storage[7], which means that, allowing hydrogen gas to react with alloy to form corresponding hydride, and lead hydrogen to be stored in the alloy matrix in atomic form, is the most promising hydrogen storage method due to its safety and high theoretical capacity[8].

Chemical hydrogen storage can be achieved through a variety of materials, including alloys[9], intermetallic compounds [10], complex hydrides[11], etc. Among intermetallic compounds, rare earth-based alloys have superior hydrogen storage properties[12]. In today's commercial fuel cells, $LaNi_5$ alloy[13] occupies a large proportion in Ni-MH cells. Meanwhile, RE-Mg-Ni alloys have attracted extensive attention due to their higher hydrogen storage capacity than $LaNi_5$. This type of alloy has a special structure and is formed by stacking A_2B_4 and AB_5 structures, and the basic expression is $m[RMgNi_4] \cdot n[RNi_5]$[14]. According to this formula, it can be obtained that RE-Mg-Ni alloys have AB_3, A_2B_7, A_5B_{19} and AB_4 types. Among them, the properties of A_2B_7 alloy and A_5B_{19} alloy are the most attractive.

Since K.Kadir[15] et al. synthesized La_4MgNi_{19} intermetallic compound, the structure and properties of this type of alloy have been studied by a large amount of scholars. The results of YimingLi[16] et al. show that the La_4MgNi_{19} intermetallic compound after casting and annealing has a maximum hydrogen storage capacity of 1.572 wt.%, a maximum discharge capacity of 355.1 mAh/g, and a HRD of 93.3% after 300 cycles. Qingan Zhang[17] et al. investigated the phase stability, structural transformation, and hydrogen absorption and desorption characteristics of La_4MgNi_{19} intermetallic compound, and it was found that in the range of 840-960 °C, there are two variants of La_4MgNi_{19} intermetallic compound, namely the stable hexagonal structure (2H) at higher temperature and the rhombohedral structure (3R) at lower temperatures. In order to optimize its performance, lots of researchers have carried out treatments such as heat treatment and element substitution. When performing element substitution, rare earth elements such as Pr[18], Sm[19], Gd[20], and Nd[21] were always used to substitute La, and Co[22] to substitute Ni. Unfortunately in these articles, the elements used are only synthesized according to the composition after the element substitution. It does not indicate that element substitution has actually occurred, what it indeed means is, only nominal element substitution has been carried out. Moreover, few literatures have considered theoretical calculations on La_4MgNi_{19}. Proper theoretical calculations[23] can be applied to explain the transform in properties after substitution of various elements more intuitively and in more details.

In this work, the single-element substitution of La_4MgNi_{19} intermetallic compound was researched by first principles density functional theory calculation. In the calculation, Pr, Sm, Gd and Nd elements were employed to substitute La and Co to substitute Ni through the total energy calculation, the positions preferentially occupied by the substitution elements were determined, and the variation rule of the formation enthalpy was revealed, which can provide guidance for the element substitution for the hydrogen storage alloys, and help reasearchers to understand the mechanism of substitution.

2. Computational models and method

Figure 1 shows the structure of La_4MgNi_{19}. Its unit cell belongs to the P63/MMC space group, and the lattice parameters are a=0.5032 nm, c=3.2223 nm. The unit cell of La_4MgNi_{19} contains 2 formula units, that is to say, the chemical formula is $La_8Mg_2Ni_{38}$. Among them, 8 La atoms occupying La(2c) and La(4f) sites, 38 Ni atoms occupy Ni(2a), Ni(2b), Ni(2d), Ni(4e), Ni(4f), Ni(12k1), Ni (12k2) site and 2 Mg atoms occupy the La(4f) site, respectively. At this site, La occupies 41.2% of each atom and Mg occupies 58.8% of each atom, all structural parameters are from the literature[8]. In order to study the case of element substitution, the aforementioned substitution atoms were introduced into the structure. In this case, one La atom or one Ni atom was substituted. Substitution atoms were sequentially introduced into different positions of La or Ni, and the corresponding total energies were calculated. In this work, the formation enthalpy is defined as the difference between the total energy and the energy of the constituent elements in the steady state. The enthalpy of formation can be used to demonstrate whether a compound is thermodynamically superior to the constituent elements, and subsequently determine which positions are preferentially occupied by these elements.

The calculation relied on the CASTEP programme, which is a first principles quantum mechanical code based on the density functional theory[24]. The Perdew–Burke–Ernzerhof (PBE) generalized gradient approximation (GGA) exchange and correlation potential were used in the calculations. In the calculation, ultrasoft pseudopotentials[24] were used for replacing the core electrons. The energy cutoff is 380 eV and the k-point sets are 6×6×2 during the process of geometry optimization calculations. The corresponding k-point sets are 6×6×2 for pure and rare earth-doped La_4MgNi_{19} unit cell. Other parameters for geometry optimization are below: convergence criteria: 5.0×10^{-6} eV/atom, maximum force: 0.01 eV/Å, maximum stress: 0.02 GPa and maximum displacement: 5.0×10^{-4} °A.

3. Results and discussion

Before the initial of calculations, the La_4MgNi_{19} lattice was fully geometrically optimized in advance, including lattice parameters and atomic coordinates. The experimental data from the literature[8] and the geometrically optimized data are contrasted in Table 1. The changed parameters are listed in the table, while the unchanged parameters, such as La(2c), Ni(2a), Ni(2b) and Ni(2d) coordinates are not listed. As can be seen from the table, in the whole data table, the maximum difference is not more than 1.6%, which can prove that the calculated data is in high agreement with the experimental data from the literature.

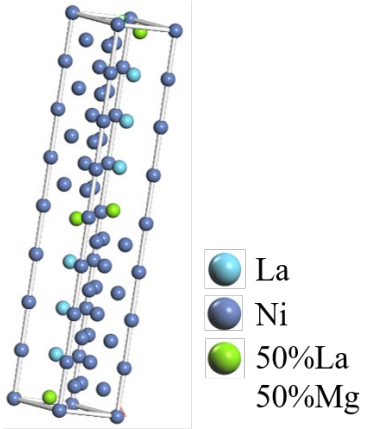

Fig. 1. The structure of La_4MgNi_{19} (shown as a unit cell, $La_8Mg_2Ni_{38}$)

The calculation of the enthalpy of formation was performed after the geometric optimization. One Pr, Sm, Gd or Nd atom was introduced to replace La, forming $La_7X_mMg_2Ni_{38}$ (m is the position of the La atom, which is La(2a) or La(4f), and X is the substitution element, which is Pr, Sm, Gd or Nd) or a Co atom is introduced into the crystal structure to replace the Ni atom at a different position and form $La_8Mg_2Ni_{37}Co_n$ (n is the different position of the Ni atom, which is Ni(2a), Ni(2b), Ni(2d), Ni(4e), Ni(4f), Ni(12k1) or Ni(12k2)).

The results are shown in Figures 2. According to Figure 2, the formation enthalpy of La_4MgNi_{19} alloy is lower than that of the four doped alloys, which indicates that the phase stability will be reduced when the four rare earth elements are separately doped into the alloy. In the formation enthalpy of La_4MgNi_{19} with four doping elements substituted for La, when La(4f) is substituted, an alloy whose enthalpy is lower than that of La(2c) position is formed, indicating that these four elements will preferentially occupy La(4f) during the element replacement process. In addition, according to the formation enthalpy, it can be judged that the order of phase stability of the substitued alloys is: Pr>Nd>Sm>Gd. The article of Li et al.[25] showed that, the cycle performance when different rare earth elements replace La. It can be found that the discharge capacity of Pr_4MgNi_{19} decays quickly after several cycles, while the capacity decay of La_4MgNi_{19} is slower, which shows that after Pr substitutes La, the stability of the structure decreases. Chen et al. research[26] showed that the maximum discharge capacity decreases and the discharge rate increases with the increase of Sm, which indicates that the phase stability decreases gradually. The experimental results of Li R et al.[27] in the electrochemical test part of the article show that as the Gd content in the alloy increases, the discharge rate of the alloy gradually increases, which indicates that the phase stability gradually decreases. Xin Z et al.[28] found when Nd is replaced and reduced, the capacity retention of HRD gradually increases, so the presence of Nd reduces the phase stability. These results show that the simulation results are highly consistent with the experimental results in the literature. As Figure 2 showed, compared with the enthalpy of formation of La_4MgNi_{19} where Co replaces Ni at any position, the enthalpy of the substrate alloy is the lowest, which shows that no matter which position of Ni Co pinnings on, the stability of La_4MgNi_{19} will be reduced. Among all the sites of Ni, the enthalpy of Co occupying Ni(12k2) is the

Table 1
Experimental[8] and calculated structural parameters of La_4MgNi_{19}

Lattice parameter			Atomic coordinates						
	experimental	calculated		experimental			calculated		
a	0.5032nm	0.5032nm	La(4f1)	1\3	2\3	0.12591	1\3	2\3	0.12793
c	3.2191nm	3.2191nm	La(4f1)	1\3	2\3	0.01687	1\3	2\3	0.01705
			Ni(4e)	0	0	0.12759	0	0	0.12539
			Ni(4f)	1\3	2\3	0.87576	1\3	2\3	0.87478
			Ni(12k1)	0.8350	2x	0.06549	0.8331	2x	0.06475
			Ni(12k2)	0.8350	2x	0.18998	0.8333	2x	0.1879

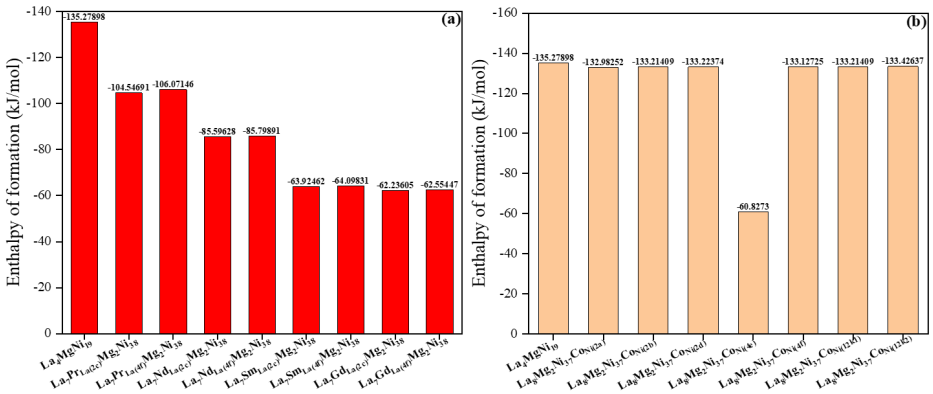

Fig.2. (a) The enthalpy of formation of La_4MgNi_{19} where La substituted by Pr, Sm, Gd or Nd; (b) The enthalpy of formation of La_4MgNi_{19} where Ni substituted by Co.

lowest, which reveals that Co will preferentially occupy the Ni(12k2) site during the process of element substitution. Liu J. et al.[14] found that the HRD would be significantly improved when Sm was substituted for La, because the addition of Sm will lead to grain refinement. Sm pinning at the grain boundaries prevents the growth of grains, at the same time the increased hydrogen storage kinetics also indicated a decrease in phase stability. The experimental results of Lu H H et al.[29] showed that Co substituting Ni would increase the discharge rate, which means a decreased stability of phase. It is also consistent with the above conclusion on structural stability[30]. The results of experiment of Wei F S et al.[31] showed that the maximum discharge capacity increases with the increase of Co, but the high-rate dischargeability decreases with the increase of Co, but the difference is not significant. This is consistent with the conclusion that the enthalpy of formation is not much different from our calculation results, but the phase stability is reduced. In conclusion, the hydrogen storage performance can be optimized by designing rational element substitution[32][33].

To discuss the effect of the substitutions at the La site on the electronic structure, the total densities of states (TDOSs)[34] are plotted in Fig. 3 for $La_7M_{(La(2c)\ or\ La(4f))}Mg_2Ni_{38}$ (M = Pr, Nd, Sm, Gd). On account to making use of the double cell model of La_4MgNi_{19}, the TDOS are twice as big as the data of the unit cell. And the Fermi level E_F[35] has been set as the zero point of the energy in every figure.

The demonstration of results of the electronic structure of pure La_4MgNi_{19} are shown below.

As shown in Figure 3(a), the main bonding peaks of La_4MgNi_{19} alloy lie in the range of -17 to -15 and -10 to E_F. In the range of -17 to -15, La P and Mg P orbitals are highly bonded, while in the range of -10 to -5, the orbitals of Mg s, Mg P, Ni s and Ni P are bonded, and in the range of - 5 to E_F, the bonding peaks of Ni d, a small amount of La d and a small amount of Mg P appeared. In summary, the orbitals of La, Mg and Ni elements are extensively hybridized. The high-strength bonding of electrons[36] in these high-energy orbitals determines the phase stability. The valence band width[37] can be calculated from the scale from the E_F in the DOS figure to the point whose vertical coordinates is 0. It is shown that the valence band width of the La_4MgNi_{19} is 10.41.

The bonding states are formed by the interaction between the hybridization orbital of atom s, p, d and f orbital[38]. In order to give a qualitative characteristics of electronic structure in these alloy, the partial density of states (PDOSs)[39] plots for La, Mg, Ni, and X (X = Pr, Gd, Nd, Sm) atoms are given in Fig. 3(b-i). It can be acquired that all of the PDOS of the elements have crossed the Fermi level E_F, which shows that after the element substitution occurs, the system of the overall material still puts up the metallic character. Compared with the valence band width of the La_4MgNi_{19} 10.41, the valence band width of rare-earth-doped La_4MgNi_{19} is increased, which are 10.96, 10.51, 10.98, 10.96, 10.91, 10.99, 10.95, 11.00 (Gd(La(2c)), Gd(La(4f)), Nd(La(2c)),

Nd(La(4f)), Pr(La(2c)), Pr(La(4f)), Sm(La(2c)), Sm(La(4f))). Among them, Sm(La(4f)) has the maximum width, which is due to the contribution of the d and f orbit of the Sm element. And then, in the energy range of -17 to E_F, the intensity of the bonding peaks of La, Mg and Ni decreases because of the involving of substitution elements. Meanwhile, in the energy range of -18 to -15 and -5 to E_F, the doping elements participate in the bonding of the original atoms. Due to the doping of the corresponding substitution elements, the original bonding peak strength is weakened, so the phase stability is weakened. In addition, for different doping elements, the energy intensity of their doping element orbitals participating in the bonding peak can determine their phase stability. The more they participate, the weaker the phase bondings are and the weaker their stability of the phases are. According to the bonding peak intensity of each doping element in the DOS diagram, it can be concluded that the order of the stability of the phases is as follows: Pr>Nd>Sm>Gd. This is in agreement with the calculated enthalpy of formation. Futhermore, for different La substitution positions, for 4 different doping elements, when the doping elements substitute on the La(4f) position, the energy values of these main bonding peaks, namely La p, Mg p, Ni d orbitals, are higher than that of the doping elements on the position of La(2c). As for the energy value of the f orbital of the doping elements, the corresponding value of La(4f)-doping alloys are lower than that of La(2c)-doping alloys, which indicates that the bonding strength of the La(4f)-doping is relatively low, revealing that the doping elements are less involved in the original bonding, so the stability of alloys are less disturbed, which equals to a high phase stability. The mentioned conclusion above is also consistent with the result of the formation enthalpy. Meanwhile, the intereaction[40] of Ni d and rare-earth f is very strong, the order of the intensity of interaction is Gd>Sm>Nd>Pr.

The bounding hydrogen capacity of the La-doped hydrides also been calculated because the application of these compounds. Through this, the theorical properties of hydrogen storage of these compounds can be obtained.

In order to explore the order of the theoretical hydrogen storage capacity for different doped elements, it must be assumed that every interstitial space that can accommodate hydrogen atom has already accommodated hydrogen atom. Therefore the full model of La_4MgNi_{19} hydrides should be built. To built it, we assumed that the space group is as same as the corresonding alloy. Owing to the structure, namely RNi_5+$RMgNi_4$, the positions of hydrogen should be considered separately. For RNi5 structure, the positions were set according to $LaNi_5H_7$[41], which include La_2Ni_2 site, Ni_4 site and La_2Ni_4 site. Meanwhile, for $RMgNi_4$, the positions of hydrogen refers to the structure of $ZrMn_2H_3$[42], which include Zr_2Mn_2 (241) site, Zr_2Mn_2 (12k) site and two Zr_2Mn_2 (6h) sites.

After building the structure, the entahlpy of formation of hydride can be obtained by the formula

$$E_{for}=E_t(La_7MMg_2Ni_{38}H_{25}) -E_t(La_7MMg_2Ni_{38})-25E_i(H) \quad (1)$$

where $E_t(La_7MMg_2Ni_{38}H_{25})$ and $E_t(La_7MMg_2Ni_{38})$ refer to the total energy of two compounds. $E_i(H)$ is the total energy of single hydrogen. E_{for} is defined as the bounding hydrogen capacity. The more negative it is, the stronger the hydrogen bounding energy, which means the more capacity.

The formation energy of hydrogen atom and total energy for the hydrides of $La_7M_{(La(2c)\ or\ La(4f))}Mg_2Ni_{38}$ (M = Pr, Nd, Sm, Gd) are listed in Table 2. The total energy of single hydrogen atom is -11.032 eV. As can be seen from Table 2, the formation energy for the hydrogen atoms in $La_8Mg_2Ni_{38}H_{25}$ is -4.3671 eV. After the substitution it increases to between 5 to 7 for $La_7MMg_2Ni_{38}$ (M = Pr, Nd, Sm, Gd). This reveals that the substitutions of La by rare earth elements could promote the bounding hydrogen capacity of the compounds. Therefore, the formation energy of hydrogen atom ordered by doped elements is Nb > Sm > Pr > Gd > base alloy. It means that the order of bounding hydrogen capacity of the substituted alloys is Nb > Sm > Pr > Gd.

Table 2

The formation energy of hydrogen atom and total energy of $La_7M_{(La(2c)\ or\ La(4f))}Mg_2Ni_{38}$ (M = Pr, Nd, Sm, Gd).

Structure	E_t (eV)	E_{for} (eV)	Structure	E_t (eV)	E_{for} (eV)
$La_8Mg_2Ni_{38}H_{25}$	-60572.5115	-4.3671	$La_7Sm_{(La(2c))}Mg_2Ni_{38}H_{25}$	-61233.7066	-6.4151
$La_7Pr_{(La(2c))}Mg_2Ni_{38}H_{25}$	-61879.1495	-6.2028	$La_7Sm_{La(4f))}Mg_2Ni_{38}H_{25}$	-61233.9578	-6.5754
$La_7Pr_{(La(4f))}Mg_2Ni_{38}H_{25}$	-61879.3403	-6.3344	$La_7Gd_{(La(2c))}Mg_2Ni_{38}H_{25}$	-60696.7329	-5.9111
$La_7Nd_{(La(2c))}Mg_2Ni_{38}H_{25}$	-62256.7413	-6.8443	$La_7Gd_{(La(4f))}Mg_2Ni_{38}H_{25}$	-60696.8708	-5.8928
$La_7Nd_{(La(4f))}Mg_2Ni_{38}H_{25}$	-62257.6297	-6.9741	/	/	/

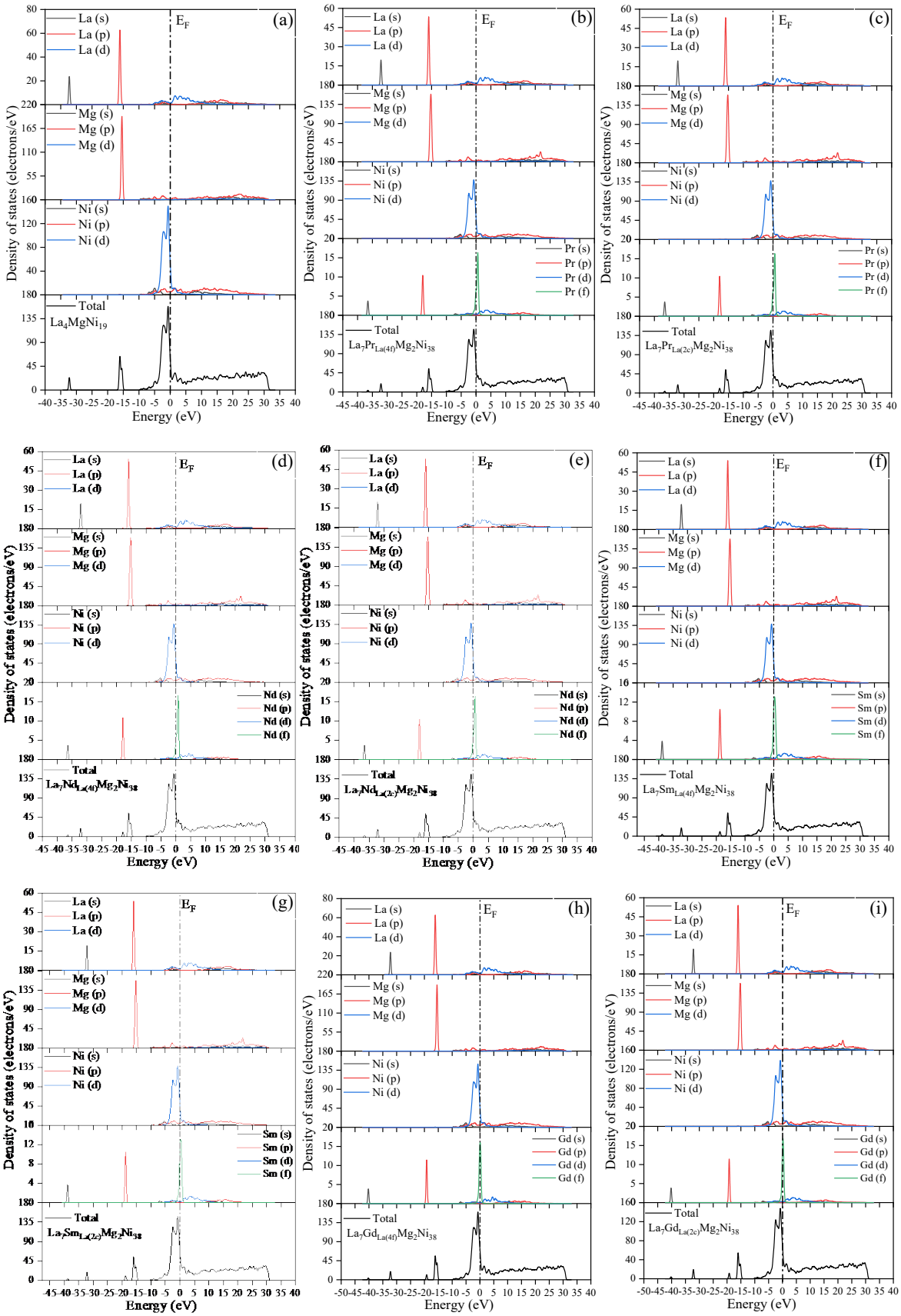

Fig.3. (a)The DOS of La_4MgNi_{19} (b)(c) The DOS of Pr-doped La_4MgNi_{19} (d)(e) The DOS of Nd-doped La_4MgNi_{19} (f)(g) The DOS of Sm-doped La_4MgNi_{19} (h)(i) The DOS of Gd-doped La_4MgNi_{19}

4. Conclusion

In this study, the first-principles density functional theory method was used to calculate the situation of element substitution of La_4MgNi_{19}, and the following conclusions were obtained: First, there is only a small difference between the model obtained after geometric optimization and the experimental data in the literature[8], indicating that the calculated results are highly consistent with the experimental results. Second, for La substitution, the situation of the substitution of other four rare-earth elements (Pr, Nd, Sm and Gd) were investiagted. The results of calculation revealed that these four elements preferentially occupy the La(4f) site. And the addition of the four doping elements will reduce the stability of the phase. Among them, Pr substituted La_4MgNi_{19} has the highest structural stability. For the substitution of Ni, no matter which position Co occupies, the structural stability will be reduced. Co preferentially occupies the Ni(12k2) site. At the same time, the above stability conclusion is also consistent with the conclusion in the existing literature. Third, the DOS study shows that the system of the overall material still puts up the metallic character. And the valence band width of Sm(La(4f)) becomes wider, which contributes by Sm d and f. The intereaction of Ni d and rare-earth f is very strong, the order of the intensity of interaction is Gd>Sm>Nd>Pr. The element orbitals of the three elements in the La_4MgNi_{19} alloy are extensively hybridized, and the doping of La reduces the phase stability, and according to the difference in energy peak heights, it can be extracted that the stability of four doped alloys from high to low is: Pr, Nd, Sm, Gd. Fourth, according to the calculation of the hydride formation enthalpy of different doping elements, the bounding hydrogen capacity of the system can be obtained as Nb > Sm > Pr > Gd.

Acknowledgement

The work was supported by China Scholarship Council (China) and UTBM (France) in the framework of UT-INSA project (2020).

References

[1] Kadir K, Sakai T, Uehara I. Synthesis and structure determination of a new series of hydrogen storage alloys; RMg2Ni9 (R= La, Ce, Pr, Nd, Sm and Gd) built from MgNi2 Laves-type layers alternating with AB5 layers[J]. Journal of Alloys and Compounds, 1997, 257(1-2): 115-121.

[2] Zandalinas S I, Fritschi F B, Mittler R. Global warming, climate change, and environmental pollution: recipe for a multifactorial stress combination disaster[J]. Trends in Plant Science, 2021, 26(6): 588-599

[3] Razmjoo A, Gandomi A H, Pazhoohesh M, et al. The key role of clean energy and technology in smart cities development[J]. Energy Strategy Reviews, 2022, 44: 100943.

[4] Abe J O, Popoola A P I, Ajenifuja E, et al. Hydrogen energy, economy and storage: Review and recommendation[J]. International journal of hydrogen energy, 2019, 44(29): 15072-15086.

[5] Usman M R. Hydrogen storage methods: Review and current status[J]. Renewable and Sustainable Energy Reviews, 2022, 167: 112743.

[6] Tarhan C, Çil M A. A study on hydrogen, the clean energy of the future: Hydrogen storage methods[J]. Journal of Energy Storage, 2021, 40: 102676.

[7] Kojima Y. Hydrogen storage materials for hydrogen and energy carriers[J]. International Journal of Hydrogen Energy, 2019, 44(33): 18179-18192.

[8] Zhao Y, Zhang L, Ding Y, et al. Comparative study on the capacity degradation behavior of Pr5Co19-type single-phase Pr4MgNi19 and La4MgNi19 alloys[J]. Journal of Alloys and Compounds, 2017, 694: 1089-1097.

[9] Marques F, Balcerzak M, Winkelmann F, et al. Review and outlook on high-entropy alloys for hydrogen storage[J]. Energy & Environmental Science, 2021, 14(10): 5191-5227.

[10] Yartys V A, Lototskyy M V. Laves type intermetallic compounds as hydrogen storage materials: A review[J]. Journal of Alloys and Compounds, 2022: 165219.

[11] Dematteis E M M, Amdisen M B, Autrey T, et al. Hydrogen storage in complex hydrides: past activities and new trends[J]. Progress in Energy, 2022.

[12] Jiang W, Chen Y, Hu M, et al. Rare earth-Mg-Ni-based alloys with superlattice structure for electrochemical hydrogen storage[J]. Journal of Alloys and Compounds, 2021, 887: 161381.

[13] Ye Y, Yue Y, Lu J, et al. Enhanced hydrogen storage of a LaNi5 based reactor by using phase change materials[J]. Renewable Energy, 2021, 180: 734-743.

[14] Liu J, Han S, Li Y, et al. Cooperative effects of Sm and Mg on electrochemical performance of La–Mg–Ni-based alloys with A2B7-and A5B19-type super-stacking structure[J]. International Journal of Hydrogen Energy, 2015, 40(2): 1116-1127.

[15] Liu J, Li Y, Han S, et al. Microstructure and electrochemical characteristics of step-wise annealed La0. 75Mg0. 25Ni3. 5 alloy with A2B7-and A5B19-type super-stacking structure[J]. Journal of The Electrochemical Society, 2013, 160(8): A1139.

[16] Wang W, Qin R, Wu R, et al. A promising anode candidate for rechargeable nickel metal hydride power battery: An A5B19-type La–Sm–Nd–Mg–Ni–Al-based hydrogen storage alloy[J]. Journal of Power Sources, 2020, 465: 228236.

[17] Zhang Q, Fang M, Si T, et al. Phase stability, structural transition, and hydrogen absorption− desorption features of the polymorphic La4MgNi19 compound[J]. The Journal of Physical Chemistry C, 2010, 114(26): 11686-11692.

[18] Li Y, Zhang Y, Ren H, et al. Mechanism of distinct high rate dischargeability of La4MgNi19 electrode alloys prepared by casting and rapid quenching followed by annealing treatment[J]. International Journal of Hydrogen Energy, 2016, 41(41): 18571-18581.

[19] Hao X, Salhi I, Laghrouche S, et al. Backstepping Super-Twisting control of Four-Phase Interleaved Boost Converter for PEM Fuel Cell[J]. IEEE Transactions on Power Electronics, 2022.

[20] Lozano F J, Gijón-Rivera M Á, Huertas-Bolaños M E. Fossil Fuels Use and Efficiency During the Transition to a Low-Carbon Economy[M]//Energy Issues and Transition to a Low Carbon Economy. Springer, Cham, 2022: 59-94.

[21] Sakintuna B, Lamari-Darkrim F, Hirscher M. Metal hydride materials for solid hydrogen storage: a review[J].

International journal of hydrogen energy, 2007, 32(9): 1121-1140.

[22] Kohno T, Yoshida H, Kawashima F, et al. Hydrogen storage properties of new ternary system alloys: La2MgNi9, La5Mg2Ni23, La3MgNi14[J]. Journal of alloys and compounds, 2000, 311(2): L5-L7.

[23] Hao X, Salhi I, Laghrouche S, et al. Multiple inputs multi-phase interleaved boost converter for fuel cell systems applications[J]. Renewable Energy, 2023.

[24] Clark S J, Segall M D, Pickard C J, et al. First principles methods using CASTEP[J]. Zeitschrift für kristallographie-crystalline materials, 2005, 220(5-6): 567-570.

[25] Li Y, Han D, Han S, et al. Effect of rare earth elements on electrochemical properties of La–Mg–Ni-based hydrogen storage alloys[J]. International journal of hydrogen energy, 2009, 34(3): 1399-1404.

[26] Chen M, Tan C, Jiang W, et al. Influence of over-stoichiometry on hydrogen storage and electrochemical properties of Sm-doped low-Co AB5-type alloys as negative electrode materials in nickel-metal hydride batteries[J]. Journal of Alloys and Compounds, 2021, 867: 159111.

[27] Li R, Wan J, Wang F, et al. Effect of non-stoichiometry on microstructure and electrochemical performance of La0. 8GdxMg0. 2Ni3. 15Co0. 25Al0. 1 (x= 0–0.4) hydrogen storage alloys[J]. Journal of Power Sources, 2016, 301: 229-236.

[28] Xin Z, Dandan K E, Liqiang J I, et al. Crystallographic and electrochemical hydrogen storage properties of Sm substitute Nd for La0. 5Nd0. 35-xSmxMg0. 15Ni3. 5 alloys[J]. Energy Storage Science and Technology, 2020, 9(4): 1066.

[29] Lu H H, Wei F S, Wei F N. The Phase Structure and Electrochemical Properties of La4MgNi19-xCox (x= 0~ 2) Hydrogen Storage Alloys[C]//Advanced Materials Research. Trans Tech Publications Ltd, 2014, 875: 277-281.

[30] Matsumura T, Yukawa H, Morinaga M. Alloying effects on the electronic structure of ZrMn2 intermetallic hydride[J]. Journal of alloys and compounds, 1998, 279(2): 192-200.

[31] Wei F S, Cai X, Zhang Y, et al. Structure and Electrochemical Properties of La4MgNi17. 5M1. 5 (M= Co, Fe, Mn) Hydrogen Storage Alloys[J]. Int. J. Electrochem. Sci, 2017, 12: 429-439.

[32] Liu Y, Yuan H, Guo M, et al. Effect of Y element on cyclic stability of A2B7-type La–Y–Ni-based hydrogen storage alloy[J]. International Journal of Hydrogen Energy, 2019, 44(39): 22064-22073.

[33] Liu J, Li Y, Han D, et al. Electrochemical performance and capacity degradation mechanism of single-phase La–Mg–Ni-based hydrogen storage alloys[J]. Journal of Power Sources, 2015, 300: 77-86.

[34] Gaspard J P, Cyrot-Lackmann F. Density of states from moments. Application to the impurity band[J]. Journal of Physics C: Solid State Physics, 1973, 6(21): 3077.

[35] Kahn A. Fermi level, work function and vacuum level[J]. Materials Horizons, 2016, 3(1): 7-10.

[36] Czapla M, Skurski P. Strength of the Lewis–Brønsted superacids containing In, Sn, and Sb and the electron binding energies of their corresponding superhalogen anions[J]. The Journal of Physical Chemistry A, 2015, 119(51): 12868-12875.

[37] Hassanien A S, Sharma I. Band-gap engineering, conduction and valence band positions of thermally evaporated amorphous Ge15-x Sbx Se50 Te35 thin films: Influences of Sb upon some optical characterizations and physical parameters[J]. Journal of Alloys and compounds, 2019, 798: 750-763.

[38] Alabugin I V, Bresch S, dos Passos Gomes G. Orbital hybridization: a key electronic factor in control of structure and reactivity[J]. Journal of Physical Organic Chemistry, 2015, 28(2): 147-162.

[39] Gasparian V, Christen T, Büttiker M. Partial densities of states, scattering matrices, and Green's functions[J]. Physical Review A, 1996, 54(5): 4022.

[40] Lang J K, Baer Y, Cox P A. Study of the 4f and valence band density of states in rare-earth metals. II. Experiment and results[J]. Journal of Physics F: Metal Physics, 1981, 11(1): 121.

[41] Thompson P, Reilly J J, Corliss L M, et al. The crystal structure of LaNi5D7[J]. Journal of Physics F: Metal Physics, 1986, 16(6): 675.

[42] Pontonnier L, Miraglia S, Fruchart D, et al. Structural study of hyperstoichiometric alloys ZrMn2+ x and their hydrides[J]. Journal of alloys and compounds, 1992, 186(2): 241-248.